Elastic Snap-Through Instabilities Are Governed by Geometric Symmetries

Basile Radisson and Eva Kanso

Elastic snap-through instabilities are governed by geometric symmetries

Basile Radisson and Eva Kanso

Department of Aerospace and Mechanical Engineering,
University of Southern California, Los Angeles, CA 90089-1191, USA
(Dated: April 18, 2023)

Many elastic structures exhibit rapid shape transitions between two possible equilibrium states: umbrellas become inverted in strong wind and hopper popper toys jump when turned inside-out. This snap-through is a general motif for the storage and rapid release of elastic energy, and it is exploited by many biological and engineered systems from the Venus flytrap to mechanical metamaterials. Shape transitions are known to be related to the type of bifurcation the system undergoes, however, to date, there is no general understanding of the mechanisms that select these bifurcations. Here we analyze numerically and analytically two systems proposed in recent literature in which an elastic strip, initially in a buckled state, is driven through shape transitions by either rotating or translating its boundaries. We show that the two systems are mathematically equivalent, and identify three cases that illustrate the entire range of transitions described by previous authors. Importantly, using reduction order methods, we establish the nature of the underlying bifurcations and explain how these bifurcations can be predicted from geometric symmetries and symmetry-breaking mechanisms, thus providing universal design rules for elastic shape transitions.

Bistability and snap-through transitions are key phenomena in many biological [1, 2] and manmade [3, 4] systems. Bistability refers to a system with two stable equilibrium states. Snap-through occurs when a system is in an equilibrium state that becomes unstable or suddenly disappears, as a control parameter is varied. Familiar examples range from the Venus flytrap [1] to children's toys [3] and ancient catapults [5]. Mechanical metamaterials, whose behavior is governed by their geometric structure rather than elastic properties, can be designed to exploit these instabilities to induce shape transitions and switch between multiple modes of functionality [6].

Elastic strips of length L, whose ends are first brought together by a distance ΔL to cause the strip to buckle into one of two stable shapes (Fig. 1A, Movie S1), then driven by boundary actuation, provide an intuitive system to demonstrate shape transitions (Figs. 1 and 2, Movies S2 and S3) [4, 7]. Starting from the Euler-buckled strip with clamped-clamped (CC) boundary conditions (BCs), when both ends are rotated symmetrically and held at a non-zero angle α, one equilibrium takes an 'inverted' shape while the other maintains its 'natural' shape. A larger rotation causes the inverted shape to snap to the natural shape. Rotating only one end also creates a violent snap-through, albeit of different character [4]. A clamped-hinged (CH) strip with the hinged end free to rotate in place and the clamped end sheared by a distance d in the direction transverse to the buckled shape exhibits snap-through [7]. A similar set-up with CC BCs leads to graceful merging of the two equilibrium states.

Despite the relative simplicity of realizing these transitions experimentally [4, 7], an understanding of how shape transitions are selected remains lacking. In a beautiful analysis, [4] showed that snap-through in asymmetric BCs arises from a saddle-node bifurcation and argued that in the case of symmetric BCs, it results from a sub-

critical pitchfork bifurcation, without explaining what leads to this change in the character of the bifurcation as BCs change. In [7], the authors alluded to similarities between their system and that of [4]. However, to date, no general theory exists for designing systems that achieve or avoid a specific type of transition. Here, we combine numerical and analytical methods to reveal the mechanisms governing shape transitions in boundary-actuated elastic strips, and we prove that the two systems in [4, 7] are equivalent. Importantly, to predict the type of bifurcation and establish design rules for creating a desired shape transition, we show that these transitions are governed by geometric symmetries.

Symmetry is one of the most fundamental concepts in physics. Symmetries shape the energy landscape and govern the equilibrium configurations the system can adopt. Broken symmetries are often invoked to explain transitions in a range of physical systems from condensed matter physics [8] to quantum field theory [9], turbulence theory [10], fluid dynamics [11], biological locomotion [12, 13], and combustion phenomena [14]. Simple one-dimensional (1D) examples from bifurcation theory show that a broken symmetry can turn a graceful pitchfork bifurcation into a violent saddle-node bifurcation (SI [15], §S1), [16]. Extending this understanding to infinite-dimensional systems is challenging to researchers and educators alike. The understanding we develop for elastic strips could thus serve as an educational tool to illustrate the role of symmetry-breaking in the bifurcation of continuum systems.

We investigate the bifurcation behavior of the elastic strips introduced in [4, 7] numerically (Figs 1–2), by leveraging the three-dimensional (3D) Cosserat theory [17], and its discrete counterpart, the Discrete Elastic Rod [18] (SI [15], §S2). To establish bifurcation diagrams and carry out asymptotic analysis, we also analyze the strip's behavior in the limit of small deflection $w(x, t)$,
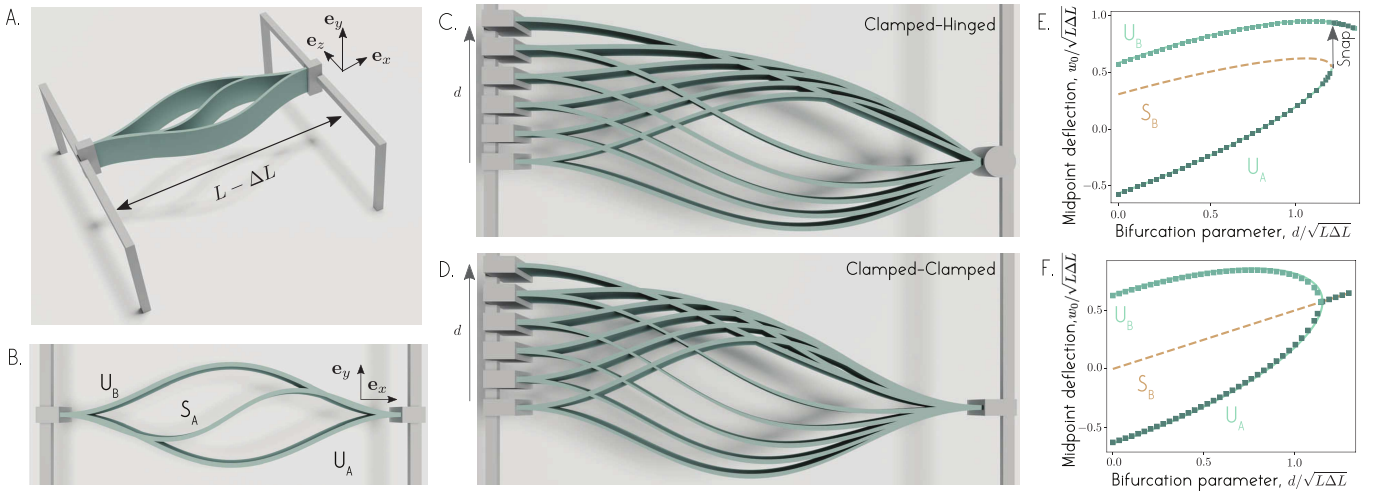
Figure 1. (A,B) **Elastic buckled strip** with clamped-clamped boundary conditions exhibits two symmetric stable equilibria U_A and U_B, and pairs of unstable equilibria of alternating symmetry at increasing energy levels, S_A and S_B denoting the first unstable pair (S_B not shown). (C-F) **Actuation of buckled strip** by (quasi-statically) translating its left end by a distance d leads to loss of bistability and a shape transition that depends on BCs: (C,E) CH strip exhibits a violent snap-through, (D,F) the transition in the CC strip is smooth. (A-D) 3D computer graphics rendering of the Cosserat numerical simulations. (E,F) midpoint deflection $w/\sqrt{L\Delta L}$ versus bifurcation parameter $d/\sqrt{L\Delta L}$. In all figures, (green) square markers represent data obtained based on the Cosserat rod theory. Solid (green) and dashed (brown) lines represent, respectively, stable and unstable branches obtained from the Euler beam model.

with $-L/2 < x < L/2$, based on the Euler-Bernoulli Beam theory ([3, 4], and SI [15], §S2),

$$\rho bh\frac{\partial^2 w}{\partial t^2} + B\frac{\partial^4 w}{\partial x^4} + F\frac{\partial^2 w}{\partial x^2} = 0. \tag{1}$$

The material properties of the strip are denoted by ρ (density), b (width), h (thickness), and $B = Ebh^3/12$ (bending stiffness, with E the Young's modulus). The applied compressive load is denoted by F. In this limit, the inextensibility condition gives rise to the nonlinear constraint equation

$$\int_{-L/2}^{L/2} \left(\frac{\partial w}{\partial x}\right)^2 dx = 2\Delta L. \tag{2}$$

The Euler-buckled strip (Fig. 1A,B) admits an infinite family of static equilibria that come in pairs, ordered by increasing value of elastic bending energy $\mathcal{E}_b$ (SI [15], §S4). We refer to members of the same pair as *twin solutions*. The fundamental buckling mode, i.e., lowest energy level, corresponds to two stable U-shape equilibria (U_A and U_B). Higher modes are unstable and alternate between odd and even harmonics. The first unstable mode gives rise to a twin of S-shape equilibria labeled S_A and S_B.

Through systematic numerical experiments, we investigate how boundary actuation modifies the U_A and U_B equilibria. In Fig. 1, we control the transverse distance d at the clamped end of the CH and CC strip (SI [15], §S5). In Fig. 2, we control the rotation at one or both ends of the CC strip by specifying the tangent direction (angle α) at the boundaries (SI [15], §S6). The control

parameters are varied incrementally starting from the twin solutions $U_{A,B}$, allowing the elastic strip to reach mechanical equilibrium at each increment. In Fig. 1E,F and Fig. 2D-F, we plot the strip's midpoint deflection w, normalized by the length scale $\sqrt{L\Delta L}$, as a function of the non-dimensional control parameters $d/\sqrt{L\Delta L}$ and $\alpha\sqrt{L/\Delta L}$, respectively. Bistability is lost beyond a certain threshold in all cases, but the character of this transition depends on boundary actuation. Asymmetric and symmetric rotations cause snap-through from the inverted (U_A) to the natural (U_B) shape, as does transverse shearing of the CH strip. The dynamic evolution of the strip differs during snapping: the displacement of the midpoint grows quadratically in time in the asymmetric case, while it grows exponentially in time in the symmetric case [19]. Antisymmetric rotations and transverse shearing of the CC strip induce graceful merging of the equilibrium shapes $U_{A,B}$. These findings are consistent with experimental observations [4, 7], and agree quantitatively with [4].

To understand the mechanisms leading to the similarities and differences in these shape transitions, we solved Eqs. (1-2) to arrive at analytic expressions for the infinite set of twin equilibria for each type of boundary actuation, and we assessed their linear stability subject to small perturbations (SI [15], §S2-S5). This analysis matches quantitatively the numerical solutions in Figs. 1E,F and 2D-F for small ΔL, and shows that, depending on the type of boundary actuation, the stable equilibrium U_A that is energetically unfavored by the boundary actuation must collide with one or both unstable $S_{A,B}$ equilibria at the shape transition.
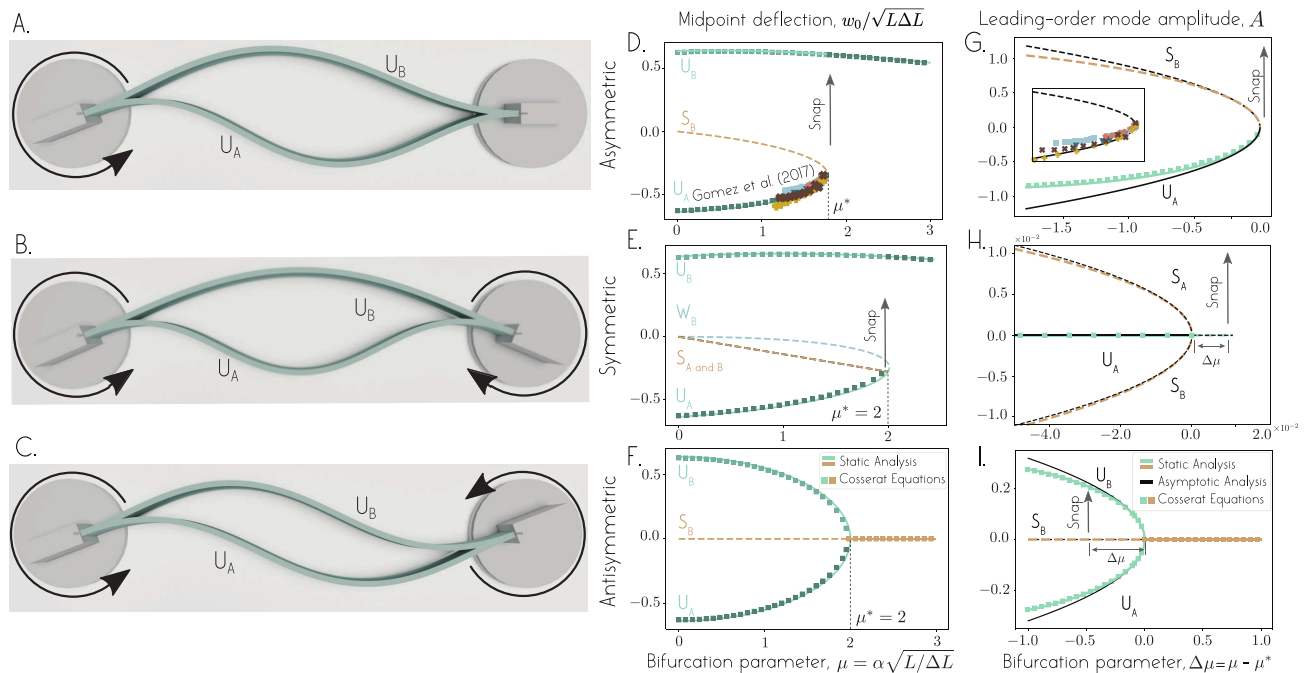
Figure 2. **Boundary actuation and bifurcation diagrams** from (quasi-statically) rotating one or both clamped ends in (A) asymmetric, (B) symmetric and (C) antisymmetric fashion. (D-F) Midpoint deflection as a function of bifurcation parameter $\mu = \alpha\sqrt{L/\Delta L}$. Experimental data from [4] are superimposed. (G-I) Asymptotic analysis near the bifurcation point μ^* gives access to normal forms describing the amplitude $A(t)$ of the leading order mode. Bifurcation diagrams of the normal forms (black lines) agree quantitatively with data obtained from the Euler beam equations (green and brown lines) and Cosserat simulations (green and brown square markers), and experimental data.

Importantly, the similarity of the bifurcation diagrams in Figs. 1 and 2 is not a coincidence. We proved, by introducing a frame of reference attached to the line connecting the strip's endpoints, that transverse shearing of the strip is equivalent to rotation of its boundaries (SI [15], §S8). Hereafter, we use the strip actuated by rotating its endpoints, with $\mu = \alpha\sqrt{L/\Delta L}$ as the bifurcation parameter, when discussing geometric symmetries and the role they play in selecting the type of bifurcation underlying a shape transition.

So which symmetries matter? Three symmetries are important and best introduced in the context of the Euler-buckled strip at $\mu = 0$: top-bottom reflection $(w \rightarrow -w)$, left-right reflection $(x \rightarrow -x)$, and π-rotation $(w \rightarrow -w$ and $x \rightarrow -x)$. Eqs. (1-2) are invariant under all three transformations (SI [15], §S3). Because the state of the system is infinite dimensional, we calculate the bending energy $\mathcal{E}_b = (EI/2) \int_{-L/2}^{L/2} (\partial^2 w/\partial x^2)^2 dx$ at $U_{A,B}$ and $S_{A,B}$ and depict the energy landscape semi-schematically on a reduced 2D space consisting of the deflection w evaluated at the strip's mid- and quarter-length (Fig. 3A; SI [15], §S10). In Fig. 3B, we unfold the energy landscape along the closed black curve connecting the U- and S-shapes. This representation highlights two important properties at $\mu = 0$: the minimum energy barrier – difference in $\mathcal{E}_b$ between $S_{A,B}$ and $U_{A,B}$ – that the strip needs to overcome in order to undergo a shape

transition from U_A to U_B, and the geometric symmetries that map U_A to U_B and S_A to S_B, and vice-versa. Specifically, the left-right symmetry maps each U-solution to itself and the top-bottom and π-rotation symmetries map a U-solution to its twin, whereas the π-rotation symmetry maps each S-solution to itself and the top-bottom and left-right symmetries map an S-solution to its twin. Hereafter, we refer to the π-rotation that maps the U-twin shapes to one another as the *U-twin symmetry* and the left-right reflection that maps the S-twin shapes to one another as the *S-twin symmetry*. The type of shape transition the system undergoes for $\mu \neq 0$ is directly related to which twin symmetry gets broken by boundary actuation.

Asymmetric boundary actuation breaks both U- and S-twin symmetries. It requires U_A to bend more than U_B and S_A to bend more than S_B, thus increasing the bending energy of U_A and S_A and decreasing that of U_B and S_B (Fig. 3C). This causes U_A and S_B to monotonically approach each other until they merge and suddenly vanish. The system must jump to U_B. Symmetric actuation breaks the U-twin symmetry but conserves the S-twin symmetry. It requires U_A to bend more than U_B but it equally affects S_A and S_B. Thus, S_A and S_B remain energetically equivalent while the energetic state of U_A increases and approaches that of S_A and S_B until they all merge in a single unstable equilibrium (Fig. 3D),
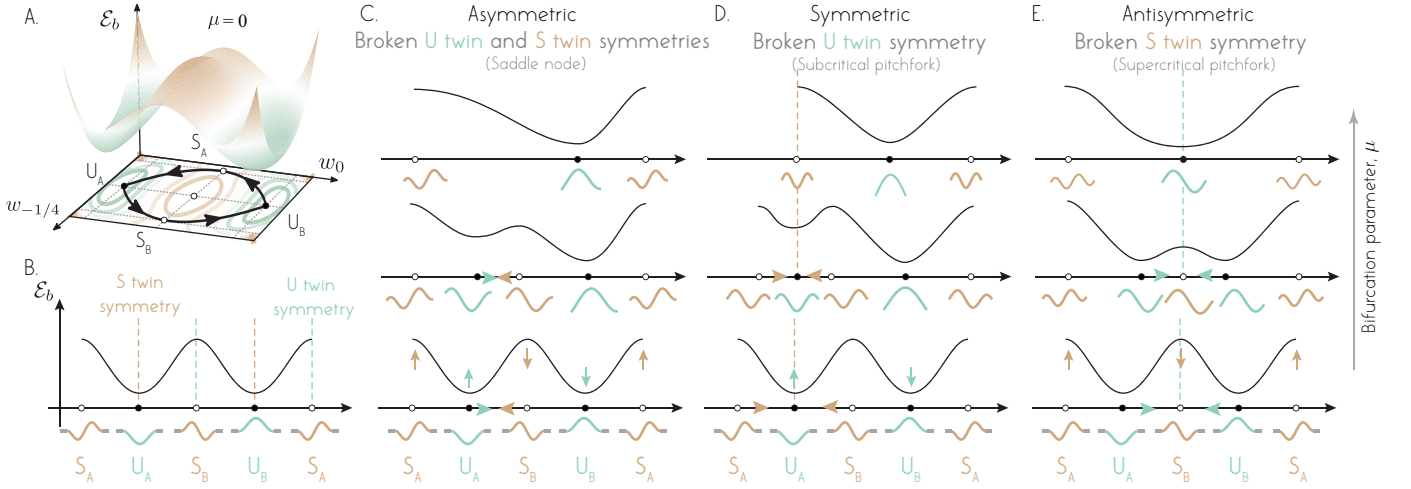
Figure 3. (A) **Energy landscape** at $\mu = 0$: two potential wells at the two stable equilibria $U_{A,B}$ separated by lowest energy barriers at the first pair of unstable equilibria $S_{A,B}$. The two paths connecting U_A to U_B via either S_A or S_B constitutes the energetically cheapest routes to pass from U_A to U_B. (B) 1D periodic representation of energy landscape. (C-E) Rotating one or both of the boundaries reshapes the energy landscape: breaking both U- and S-twin symmetries leads to a saddle-node bifurcation; breaking either U- or S-twin symmetry leads to a pitchfork bifurcation.

leaving the system no option but to jump to U_B. Antisymmetric actuation conserves the U-twin symmetry but not the S-twin symmetry: U_A and U_B remain energetically equivalent while S_A bends more than S_B; U_A and U_B monotonically approach S_B until they all gracefully merge in a single stable equilibrium (Fig. 3E).

This intuitive understanding of geometric symmetries is substantiated by extending the asymptotic analysis of [4] to derive normal forms near the shape transition at μ^*. We set $\mu = \mu^* + \Delta\mu$ with $\Delta\mu \ll 1$, and introduce the dimensionless variables $X = x/L$, $W = w/\sqrt{L\Delta L}$, $W_{eq}^* = w_{eq}^*/\sqrt{L\Delta L}$, $T = t\sqrt{B/\rho bh L^4}$ and $\Lambda^2 = FL^2/B$. To analyze the dynamic of the strip near the bifurcation, we define a slow time scale $\tau = \Delta\mu^a T$, and expand the dynamic state of the strip in powers of $\Delta\mu$ [4, 19],

$$W(X,\tau) = W_{eq}^*(X) + \Delta\mu^b W_0(X,\tau) + \text{h.o.t.},$$
$$\Lambda(\tau) = \Lambda_{eq}^* + \Delta\mu^c \Lambda_0(\tau) + \text{h.o.t.} \quad (3)$$

Here, the values of a, b, and c depend on the intrinsic properties of the system. In [19], we present a systematic approach to calculate them. We find that, for the asymmetric BCs, $a = 1/4$, $b = c = 1/2$ as postulated in [4], whereas for the symmetric and antisymmetric BCs, $a = b = 1/2$, and $c = 1$. We substitute a, b, and c into (3) and write $\Delta\mu^b W_0 = A(T)\Phi_0(X)$, where $\Phi_0(X)$ is the shape of the leading order mode and $A(T)$ its unscaled amplitude. We arrive at a reduced form for each boundary actuation (see [19]). For the asymmetric BCs, the normal form obtained in [4] is representative of a saddle node bifurcation

$$\frac{d^2 A}{dT^2} = a_{1,\text{asym}}\Delta\mu + a_{2,\text{asym}}A^2, \quad (4)$$

where $a_{1,\text{asym}}$ and $a_{2,\text{asym}}$ are positive constants (explicit expressions in [4, 19]). For the symmetric and antisymmetric BCs, we obtain a normal form representative of a pitchfork bifurcation (explicit expressions of $b_{1,(\cdot)}$ and $b_{2,(\cdot)}$ in [19],

$$\frac{d^2 A}{dT^2} = b_{1,(\cdot)}\Delta\mu A + b_{2,(\cdot)}A^3. \quad (5)$$

For the symmetric case, the coefficients $b_{1,\text{sym}}$ and $b_{2,\text{sym}}$ are positive, and the cubic term is destabilizing (subcritical pitchfork), whereas for the antisymmetric case, the coefficients $b_{1,\text{anti}}$ and $b_{2,\text{anti}}$ are negative and the cubic term is stabilizing (supercritical pitchfork).

Bifurcation analysis of (4) and (5) recapitulates the results in Fig. 3. For $\Delta\mu < 0$, (4) admits a stable equilibrium (representing U_A) and an unstable equilibrium (representing S_B) that collide and annihilate at $\Delta\mu = 0$ (Fig. 2G). As U_A vanishes, the strip is forced to snap to U_B (not represented in the reduced form). For $\Delta\mu < 0$, (5) admits three equilibria. In the symmetric case, these equilibria represent U_A, S_A, and S_B, that merge at $\Delta\mu = 0$ (Fig. 2H). U_A becomes unstable and the strip is forced to snap to U_B. In the antisymmetric case, the three equilibria represent U_A, U_B, and S_B. They merge at $\Delta\mu = 0$ (Fig. 2I). The simultaneous shape change from U_A and U_B to S_B is graceful.

To quantitatively compare this asymptotic analysis to the data in Fig. 2D-E, we calculated the amplitude A directly from data (SI [15], §S9) and plotted the results in Fig. 2G-I as a function of the distance from the bifurcation $\Delta\mu$, measured from the respective μ^* value. We observe good agreement (near μ^*) with the bifurcation diagrams of the normal forms (black lines). Notably, the reduced forms capture correctly, not only the static
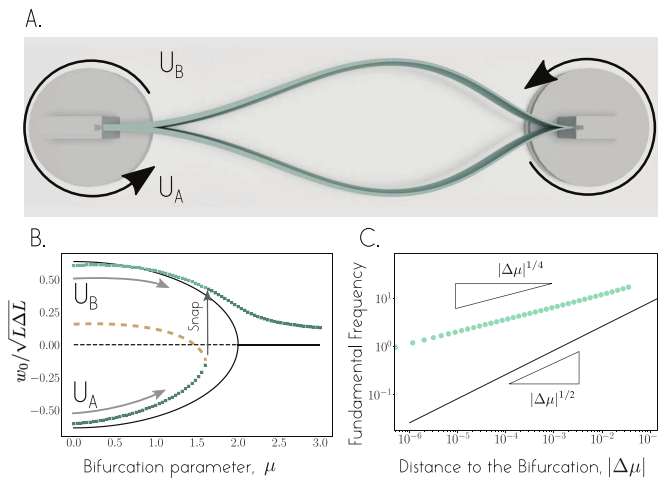
Figure 4. (A) **Tapered elastic strip** under antisymmetric boundary rotation. (B) Midpoint deflection (green symbols) versus bifurcation parameter exhibits snap-through as opposed to the graceful merging of a homogeneous strip subject to the same actuation (black lines). (C) Critical slowing down near the bifurcation scales as $(\Delta\mu)^{1/4}$ as in the case of a saddle-node.

near these bifurcations [4, 19].

The normal forms in (4) and (5) provide the backbone for plotting schematically the energy landscapes in Fig. 3D-F, which exhibit all the features of the rigorous bifurcation analysis (SI [15], §S10). Importantly, the well known symmetry breaking mechanism that turns a pitchfork into a saddle node bifurcation [16] (SI [15], §S1), appears here, in an infinite dimensional system, governing elastic transitions. This intuitive yet universal understanding of elastic instabilities based on symmetries of the Euler-buckled strip provides powerful tools for diagnostics and design. It helps explain the force hysteresis observed in [7] (SI [15], §S7). It can also help design programmable meta-materials with tunable bistability and rapid (algebraic or exponential) actuation capabilities. For a buckled elastic strip, clamped at both ends and driven via antisymmetric rotations, to undergo a nonlinear snap-through, we must break the U-twin symmetry. This can be achieved by using a strip with geometric or material heterogeneity, such as a geometrically-tapered strip instead of a homogeneous strip (Fig. 4, SI [15], §S11). Future work will consider extensions of this analysis to elastic shells and origami-based structures [20].

shape bifurcations, but also the dynamics of snapping

[1] Y. Forterre, J. M. Skotheim, J. Dumais, and L. Mahadevan, How the venus flytrap snaps, Nature **433**, 421–425 (2005).

[2] M. Smith, G. Yanega, and A. Ruina, Elastic instability model of rapid beak closure in hummingbirds, Journal of Theoretical Biology **282**, 41–51 (2011).

[3] A. Pandey, D. E. Moulton, D. Vella, and D. P. Holmes, Dynamics of snapping beams and jumping poppers, EPL (Europhysics Letters) **105**, 24001 (2014).

[4] M. Gomez, D. Moulton, and D. Vella, Critical slowing down in purely elastic 'snap-through' instabilities, Nature Physics **13**, 142–145 (2017).

[5] W. Soedel and V. Foley, Ancient catapults, Scientific American **240**, 150–161 (1979).

[6] J. L. Silverberg, A. A. Evans, L. McLeod, R. C. Hayward, T. Hull, C. D. Santangelo, and I. Cohen, Using origami design principles to fold reprogrammable mechanical metamaterials, Science **345**, 647–650 (2014).

[7] T. G. Sano and H. Wada, Snap-buckling in asymmetrically constrained elastic strips, Physical Review E **97**, 013002 (2018).

[8] P. M. Chaikin and T. C. Lubensky, *Principles of condensed matter physics* (Cambridge University Press, 1995).

[9] M. Peskin, *An introduction to quantum field theory* (CRC press, 2018).

[10] U. Frisch, *Turbulence: the legacy of A.N. Kolmogorov* (Cambridge University Press, 1996).

[11] J. D. Crawford and E. Knobloch, Symmetry and symmetry-breaking bifurcations in fluid dynamics, Annual Review of Fluid Mechanics **23**, 341–387 (1991).

[12] S. Michelin and E. Lauga, Efficiency optimization and symmetry-breaking in a model of ciliary locomotion, Physics of Fluids **22**, 111901 (2010).

[13] E. Tjhung, D. Marenduzzo, and M. E. Cates, Spontaneous symmetry breaking in active droplets provides a generic route to motility, Proceedings of the National Academy of Sciences **109**, 12381–12386 (2012).

[14] G. Joulin and P. Vidal, Flames, shocks and detonation, Hydrodynamics and Nonlinear Instabilities (ed. C. Godreche & P. Manneville) , 546–568 (1998).

[15] See Supplemental Material which includes Refs. [3, 4, 7, 16, 18, 19, 21–24], .

[16] S. H. Strogatz, *Nonlinear dynamics and Chaos: with applications to physics, biology, chemistry, and engineering*, Studies in nonlinearity (Addison-Wesley Pub, 1994).

[17] E. Cosserat and F. Cosserat, *Théorie des corps déformables* (A. Hermann et fils, 1909).

[18] M. Gazzola, L. H. Dudte, A. G. McCormick, and L. Mahadevan, Forward and inverse problems in the mechanics of soft filaments, Royal Society Open Science **5**, 171628 (2018).

[19] B. Radisson and E. Kanso, Dynamic behavior of elastic strips near shape transition, Physical Review E (2023).

[20] A. Reid, F. Lechenault, S. Rica, and M. Adda-Bedia, Geometry and design of origami bellows with tunable response, Physical Review E **95**, 013002 (2017).

[21] S. P. Timoshenko and J. M. Gere, *Theory of elastic stability* (Courier Corporation, 2009).

[22] A. H. Nayfeh and S. A. Emam, Exact solution and stability of postbuckling configurations of beams, Nonlinear Dynamics **54**, 395–408 (2008).

[23] P. Howell, G. Kozyreff, and J. Ockendon, *Applied solid mechanics*, 43 (Cambridge University Press, 2009).

[24] M. Gomez, *Ghosts and bottlenecks in elastic snap-through*, Ph.D. thesis, University of Oxford / University of Oxford (2018).